

1 **Title:** High concordance between hippocampal transcriptome of the intraamygdala kainic  
2 acid model and human temporal lobe epilepsy

3

4 **Running Title:** mRNA transcriptome in experimental and human epilepsy

5

6 Giorgia Conte<sup>1#</sup>, Alberto Parras<sup>1,2,3,4#</sup>, Mariana Alves<sup>1</sup>, Ivana Ollà<sup>3,4</sup>, Laura de Diego-Garcia<sup>1</sup>,  
7 Edward Beamer<sup>1</sup>, Razi Alalqam<sup>1</sup>, Alejandro Ocampo<sup>2</sup>, Raúl Mendez<sup>5,6</sup>, David C. Henshall<sup>1,7</sup>,  
8 José J. Lucas<sup>3,4</sup> and Tobias Engel<sup>1,7\*</sup>

9 # contributed equally

10

11 **Affiliations:**

12 <sup>1</sup>Department of Physiology & Medical Physics, Royal College of Surgeons in Ireland, Dublin  
13 D02 YN77, Ireland

14 <sup>2</sup>Department of Biomedical Sciences, Faculté de Biologie et Médecine, Université de  
15 Lausanne, Lausanne, Switzerland

16 <sup>3</sup>Centro de Biología Molecular 'Severo Ochoa' (CBMSO) CSIC/UAM, Madrid, Spain

17 <sup>4</sup>Networking Research Center on Neurodegenerative Diseases (CIBERNED), Instituto de  
18 Salud Carlos III, Madrid, Spain

19 <sup>5</sup>Institute for Research in Biomedicine (IRB), Barcelona Institute of Science and Technology,  
20 Barcelona, Spain

21 <sup>6</sup>Institució Catalana de Recerca i Estudis Avançats (ICREA), Barcelona, Spain

22 <sup>7</sup>FutureNeuro, SFI Research Centre for Chronic and Rare Neurological Diseases, RCSI,  
23 Dublin D02 YN77, Ireland

24

25 \***Correspondence:** Tobias Engel, Ph.D., Department of Physiology & Medical Physics, Royal  
26 College of Surgeons in Ireland, 123 St. Stephen's Green, Dublin 2, Ireland.

27 Tel: +35314025199 Fax: +35314022447, Email: [tengel@rcsi.ie](mailto:tengel@rcsi.ie)

28

29 **Keywords:** Status Epilepticus; Epilepsy; Transcriptome; Mouse model; Calcium signalling;  
30 CREB

31

32 Number of text pages, 26 ; Number of words, 3998; Number of references, 49; Number of  
33 Figures, 4; Number of Tables, 1; ORCID number for the first and senior authors: Tobias  
34 Engel (0000-0001-9137-0637), Alberto Parras (0000-0003-0999-2600), Giorgia Conte (0000-  
35 0003-0566-9339)

36

37

38

39

40

41

42

43

44

45

46

47

48

49

50 **Abstract**

51 *Objective:* Pharmacoresistance and the lack of disease-modifying actions of current anti-  
52 seizure drugs persist as major challenges in the treatment of epilepsy. Experimental models of  
53 chemoconvulsant-induced status epilepticus remain the models of choice to discover potential  
54 anti-epileptogenic drugs but doubts remain as to the extent to which they model human  
55 pathophysiology. The aim of the present study was to compare the molecular landscape of the  
56 intraamygdala kainic acid model of status epilepticus in mice with findings in resected brain  
57 tissue from patients with drug-resistant temporal lobe epilepsy (TLE).

58 *Methods:* Status epilepticus was induced via intraamygdala microinjection of kainic acid in  
59 C57BL/6 mice and gene expression analysed via microarrays in hippocampal tissue at acute  
60 and chronic time-points. Results were compared to reference datasets in the intraperitoneal  
61 pilocarpine and intrahippocampal kainic acid model and to human resected brain tissue  
62 (hippocampus and cortex) from patients with drug-resistant TLE.

63 *Results:* Intraamygdala kainic acid injection in mice triggered extensive dysregulation of gene  
64 expression which was ~3-fold greater shortly after status epilepticus (2729 genes) when  
65 compared to epilepsy (412). Comparison to samples of patients with TLE revealed a  
66 particular high correlation of gene dysregulation during established epilepsy. Pathway  
67 analysis found suppression of calcium signalling to be highly conserved across different  
68 models of epilepsy and patients. CREB was predicted as one of the main up-stream  
69 transcription factors regulating gene expression during acute and chronic phases and  
70 inhibition of CREB reduced seizure severity in the intraamygdala kainic acid model.

71 *Significance:* Our findings suggest the intraamygdala kainic acid model faithfully replicates  
72 key molecular features of human drug-resistant temporal lobe epilepsy and provides potential  
73 rationale target approaches for disease-modification through new insights into the unique and  
74 shared gene expression landscape in experimental epilepsy.

75 ***Key point box:***

- 76       • More genes show expression changes shortly following intraamygdala kainic acid-
- 77       induced status epilepticus when compared to established epilepsy.
- 78       • The intraamygdala kainic acid mouse model mimics closely the gene expression
- 79       landscape in the brain of patients with temporal lobe epilepsy.
- 80       • Supressed calcium signalling in the brain as common feature across experimental
- 81       models of epilepsy and patients with temporal lobe epilepsy.
- 82       • CREB is a major up-stream transcription factor during early changes following status
- 83       epilepticus and once epilepsy is established.

84

85

86

87

88

89

90

91

92

93

94

95

96

97

98

99

## 100 **Introduction**

101 A major challenge in epilepsy is the lack of adequate treatment with >30% of patients  
102 remaining resistant to currently available anti-seizure drugs (ASDs).<sup>1,2</sup> Moreover, ASDs may  
103 cause severe adverse-effects and, critically, current pharmacological treatment remains purely  
104 symptomatic and does not significantly alter the course of the disease.<sup>3</sup> Thus, there is a  
105 pressing need for the identification of drug targets with a different mechanism of action. The  
106 most common drug refractory form of epilepsy in adults is temporal lobe epilepsy (TLE)  
107 involving different structures within the limbic system, including the amygdala and  
108 hippocampus.<sup>4</sup> Pathological processes occurring during epileptogenesis include structural and  
109 functional changes such as ongoing neurodegeneration and reorganization of neural  
110 networks.<sup>5</sup> Mounting data obtained via gene expression profiling suggests these processes are  
111 driven in part by large-scale changes in the gene expression landscape within the brain.<sup>6-14</sup>

112 Whereas animal models of acute seizures (*e.g.*, pentylenetetrazol and maximal  
113 electroshock) have been successful in the identification of ASDs, the identification of anti-  
114 epileptogenic drugs and drugs to treat refractory epilepsy most likely requires different  
115 models that phenocopy the chronic stage of the disease.<sup>15</sup> The translational value of a model  
116 depends, however, on there being extensive homology with the human pathophysiology or  
117 we risk developing ineffective treatments. Currently, rodent models of status epilepticus (SE)  
118 remain the preferred method for generating drug-resistant epilepsy. The extent to which these  
119 match the molecular landscape of human refractory TLE remains uncertain. The  
120 intraamygdala kainic acid (IAKA) model of focal-onset SE in mice produces unilateral  
121 pathology and drug-resistant epilepsy after a short latent period.<sup>16</sup> The model is increasingly  
122 used for studying mechanisms of epileptogenesis and the testing of novel anti-epileptogenic  
123 drugs.<sup>17-23</sup> Whereas changes in the transcriptome have been analysed shortly following SE in

124 the model,<sup>24, 25</sup> global changes in gene expression during chronic epilepsy and whether  
125 alterations in gene expression reflect changes occurring in patients remains to be established.

126 Here, we compared the gene expression profile in the IAKA mouse model with  
127 reference data from patients with drug-resistant TLE and two other models of SE as  
128 comparator. Our results reveal excellent molecular concordance between the IAKA model  
129 and human TLE and identify potential targets for disease-modifying treatments.

130

131

## 132 **Methods**

133

### 134 *Animal model of status epilepticus*

135 Animal experiments were performed in accordance with the principles of the  
136 European Communities Council Directive (2010/63/EU) and approved by the Research  
137 Ethics Committee of the Royal College of Surgeons in Ireland (RCSI) (REC 1322, 842) and  
138 the Irish Health Products Regulatory Authority (AE19127/P038). Experiments were carried  
139 out in 8-12-week-old C57Bl/6 male mice bred at RCSI.<sup>26</sup> SE was induced in fully awake  
140 mice via a microinjection of kainic acid (KA) (0.3  $\mu$ g in 0.2  $\mu$ l phosphate-buffered saline  
141 (PBS)) (Sigma-Aldrich, Dublin, Ireland) into the basolateral amygdala. Vehicle-injected  
142 control animals received 0.2  $\mu$ l PBS. The anticonvulsive lorazepam (6mg/kg) (Wyetch,  
143 Taplow, UK) was delivered i.p. 40 min post-IAKA or vehicle to curtail seizures and reduce  
144 morbidity and mortality. Electroencephalogram (EEG) was recorded from cortical implanted  
145 electrodes (Xltek recording system; Optima Medical Ltd, Guildford, UK) starting 10 min  
146 prior IAKA administration.

147

### 148 *EEG quantification and behavioral assessment of seizure severity during status epilepticus*

149 Seizures were analysed via Labchart7 (ADInstruments Ltd, Oxford, United  
150 Kingdom).<sup>27</sup> EEG total power ( $\mu\text{V}^2$ ) was analysed by integrating frequency bands from 0-  
151 100 Hz. Power spectral density heat maps were generated using Labchart7 (frequency (0-  
152 40 Hz), amplitude (0-50 mV)). Clinical behaviour were scored every 5 min for 40 min after  
153 IAKA according to a modified Racine Scale.<sup>28</sup> Score 1, immobility and freezing; Score 2,  
154 forelimb and/or tail extension, rigid posture; Score 3, repetitive movements, head bobbing;  
155 Score 4, rearing and falling; Score 5, continuous rearing and falling; Score 6, severe tonic-  
156 clonic seizures. The highest score attained during each 5 min period was recorded by an  
157 observer blinded to treatment.

158

#### 159 *Drug treatment*

160 To determine the effects of CREB1 on SE, additional mice received an  
161 intracerebroventricular (i.c.v.) infusion of 2 nmol of the CREB1 inhibitor 666-15<sup>29, 30</sup> in 2  $\mu\text{l}$   
162 volume (PBS in 0.2% Dimethyl sulfoxide) 10 min before IAKA and 60 min post-lorazepam  
163 treatment to reach a final concentration of 1 mM in the ventricle (ventricle volume was  
164 calculated as 35  $\mu\text{l}$ ).

165

#### 166 *RNA isolation and microarrays analysis*

167 Mice were sacrificed 8 h or 14 days post-SE. Ipsilateral hippocampi were quickly  
168 dissected and pooled (n = 3 per pooled sample). Total tissue RNA was extracted using the  
169 Maxwell® 16 LEV simplyRNA Tissue Kit (Promega, AS1280). RNA quantification was  
170 performed with Qubit RNA Hs Assay kit (Thermo-Fisher Scientific, Q32852) and RNA  
171 integrity QC with Agilent Bioanalyzer 2100, using RNA Nano Assay (Agilent Technologies  
172 5067-1511) and RNA Pico Assay (Agilent Technologies 5067-1513). cDNA library  
173 preparation and amplification were performed with WTA2 kit (Sigma-Aldrich) using 2-5 ng

174 of total RNA as template. cDNA was amplified for 22 cycles and purified using PureLink  
175 Quick PCR Purification Kit (Invitrogen, K310001). 8  $\mu$ g of the cDNA from each sample  
176 were fragmented and labelled with GeneChip Mapping 250K Nsp assay kit (Affymetrix,  
177 900753). Hybridization was performed as described previously<sup>31</sup> during 16 h at 45°C.  
178 Washing and staining steps were performed in the GeneAtlas Fluidics Station (Affymetrix,  
179 00-0079), following the specific script for Mouse MG-430 PM Arrays. Arrays were scanned  
180 with GeneAtlas Scanner, and CEL files were done with GeneAtlas software (Affymetrix).  
181 Processing of microarray samples was performed using R and Bioconductor.<sup>32</sup> Raw CEL files  
182 were normalized using RMA background correction and summarization. Probeset annotation  
183 was performed using Affymetrix version na35. For each gene, a linear model was used to  
184 find significant differences between IAKA- or vehicle (PBS)-treated mice. Analysis of  
185 differential expression was performed using a linear model implemented in the R package  
186 "limma"<sup>33</sup>. *P*-values were adjusted with the Benjamini and Hochberg correction. We  
187 considered one gene to be down-regulated with an adjusted *P*-value  $\leq 0.01$  and FC  $< -1.2$  and  
188 up-regulated with adjusted *P*-value  $\leq 0.01$  and FC  $> 1.2$  in at least one probe. If the same  
189 transcript showed opposite results for different probes, the transcript was considered as not  
190 changed.

191

#### 192 *RNA extraction and quantitative PCR (qPCR)*

193 RNA extraction was performed using whole hippocampi.<sup>34</sup> RNA concentration was  
194 measured via a nanodrop Spectrophotometer (Thermo Scientific, Rockford, IL, U.S.A) and  
195 absorbance determined at a ratio of 260/280. Samples with an absorbance ratio between 1.8-  
196 2.2 were considered acceptable. 500  $\mu$ g of total mRNA was used to produce cDNA by  
197 reverse transcription using SuperScript III reverse transcriptase enzyme (Invitrogen, CA,  
198 U.S.A). qPCR was performed using LightCycler 1.5 (Roche Diagnostics, GmbH, Mannheim,



199 Germany). Each reaction tube contained 2  $\mu$ l cDNA, 10  $\mu$ l SyBR green Quantitect Regent  
200 (Quiagen Ltd, Hilden, Germany), 1.25  $\mu$ M primer pair (Sigma, Dublin, Ireland) and RNase  
201 free water (Invitrogen CA, U.S.A) to a final volume of 20  $\mu$ l. Data were analysed and  
202 normalized to the expression of  $\beta$ -actin. Primers used (Sigma, Dublin, Ireland) are listed in  
203 **Table S4**.

204

#### 205 *Comparison of gene expression changes between models*

206 Overlap of differentially expressed genes between different models was analyzed  
207 using the hypergeometric distribution test. Gene profiling data of the pilocarpine mouse  
208 model (12 h and 6 weeks post-SE) was obtained from<sup>10</sup> and for the intrahippocampal KA  
209 (IHKA) model (6 h and 2 weeks post-SE) from.<sup>35</sup> Transcriptome changes in TLE patients  
210 was previously reported in<sup>14</sup> for cortical tissue samples from 86 mesial temporal lobe  
211 epilepsy (mTLE) patients vs. 75 neurologically healthy controls, and<sup>12</sup>, for sclerotic  
212 hippocampus vs. non-spiking neocortex from 10 TLE patients. Genes were considered  
213 overlapping when the representation factor (RF) was  $> 2$  and  $P < 0.05$ , and dissimilar when  
214 RF was  $< 0.5$  and  $P < 0.05$ . Complete set of genes used in our study is shown in **Table S2**.

215

#### 216 *Gene Ontology analysis*

217 Pathways analysis of up- and down-regulated genes (adj.  $P$ -value  $\leq 0.01$  and FC  $> \pm$   
218 1.2) in the IAKA model (8 h and 14 days post-SE) and of overlapping genes between IAKA  
219 model and TLE patients<sup>12</sup> were analyzed using DAVID Bioinformatics Resources 6.7, KEGG  
220 pathway annotation.<sup>36</sup> This included also the analysis of Calcium signalling pathways, down-  
221 regulated transcripts in TLE patients and different epilepsy mouse models.

222

#### 223 *IPA analysis*

224 Analysis of upstream regulators was performed applying QIAGEN's Ingenuity®  
225 Pathway Analysis (IPA®) (QIAGEN Inc., [www.qiagen.com/ingenuity](http://www.qiagen.com/ingenuity))<sup>37</sup> to genes found  
226 differentially expressed (adj. P-value < 0.01 and FC > 1.5) in the IAKA mouse model at 8 h  
227 and 14 days post-SE.

228

### 229 *Data analysis*

230 Statistical analysis was performed using SPSS 25.0 (SPSS® Statistic IBM®). Data  
231 are represented as mean ± S.E.M. (Standard Error of the Mean) with 95% confidence  
232 interval. Higher or lower points (outliers) are plotted individually or are not plotted. The  
233 normality of the data was analyzed by Shapiro-Wilk test (n < 50) or Kolmogorov-Smirnov  
234 (n > 50). Homogeneity of variance was analyzed by Levene test. For comparison of two  
235 independent groups, two-tailed unpaired t-Student's test (data with normal distribution),  
236 Mann-Whitney-Wilcoxon or Kolmogorov-Smirnov tests (non-normal distribution) was  
237 performed. Enrichment tests were carried out by using one-sided Fisher's exact test.  
238 Significance was accepted at  $P < 0.05$ .

239

### 240 *Data availability*

241 Data supporting the findings of this study are available from the corresponding  
242 authors upon reasonable request. Records have been approved and assigned GEO accession  
243 numbers; however, until the acceptance of the manuscript, these will be kept private.  
244 GSE122228 - Identification of differentially expressed genes in the hippocampus in the  
245 intraamygdala kainic acid mouse model of SE.

246

247

## 248 **Results**

249

250 ***Larger transcriptome changes following status epilepticus compared to established epilepsy***  
251 ***in intraamygdala KA-treated mice***

252 To study global changes in transcript levels following SE and during epilepsy, mRNA  
253 was extracted from ipsilateral hippocampi of mice subjected to IAKA-induced SE<sup>16</sup> at two  
254 different time-points and analysed via microarrays (total of 21549 genes). As a first time-  
255 point we chose 8 h post-SE, time-point when EEG activity usually has returned to baseline  
256 levels and first signs of seizure-induced neurodegeneration appear; however, without wide-  
257 spread cell death observed at 24 h post-SE.<sup>38</sup> As a second time-point we chose 14 days post-  
258 SE, a time-point when all mice subjected to IAKA normally experience the occurrence of  
259 spontaneous seizures.<sup>16, 19, 25</sup> To reduce inter-sample variability, each sample analysed was a  
260 pool of three ipsilateral hippocampi (**Fig. 1A**). Genes were considered as differentially  
261 expressed when the adjusted *P*-value was  $\leq 0.01$  and fold change (FC)  $< -1.2$  for down-  
262 regulated and FC  $> 1.2$  for up-regulated transcripts (**Fig. 1B, Table S1**). A set of transcripts  
263 were also validated via qRT-PCR, which confirmed the microarray findings for *Hspa1b*, *Atf4*,  
264 *Ctsz* and *Laptm5* (**Fig. S1A,B**).

265 The greatest fold changes in gene expression post-SE were found for known activity-  
266 regulated transcripts including *c-Fos* (FC = 58.1) and *Inhb* (FC = 33.2). The most down-  
267 regulated transcripts were *Hes5* (FC = -6.8) and *Gpr12* (FC = -4.0) (**Fig. 1C**). A similar  
268 number of genes were up- (1366) and down-regulated (1363) post-SE. In contrast, during  
269 epilepsy, genes were mainly up-regulated (331) with only 81 genes down-regulated (**Fig.**  
270 **1D**). Furthermore, more genes showed alterations of their mRNA levels following SE (2729  
271 genes, 12.6%) when compared to established epilepsy (412 genes, 1.9%) (**Fig. 1D,E**).  
272 Finally, a very significant overlap was found between genes up- and down-regulated in the  
273 same direction at both time-points (**Fig. 1F**).

274 Taken together, our results show that IAKA-induced SE leads to a unique expression  
275 profile during SE and epilepsy with changes in mRNA levels being more prominent post-SE  
276 when compared to established epilepsy.

277

278 *The intraamygdala KA mouse model mimics the hippocampal gene expression profile of*  
279 *TLE in humans*

280 Chemoconvulsant-induced SE is one of the most common strategies to identify novel  
281 anti-epileptic drugs with KA and pilocarpine being the most frequently used.<sup>15</sup> In order to  
282 establish whether gene expression changes are similar between models, we compared  
283 transcriptome profiles of the IAKA mouse model with transcriptome changes reported for  
284 other models where epilepsy is induced via SE including the IHKA mouse model<sup>35</sup> and the i.p.  
285 pilocarpine mouse model<sup>10</sup> (**Table S2**). This revealed a similar expression pattern between  
286 the IAKA and i.p. pilocarpine mouse model at both time-points, post-SE and during epilepsy,  
287 with expression changes being more similar during established epilepsy (**Fig. 2A**). Notably,  
288 the IAKA and IHKA mouse model showed an almost complete overlap in gene expression at  
289 both time-points, post-SE and epilepsy (**Fig. 2B**).

290 Next, to determine the extent to which mRNA changes occurring in mouse models are  
291 translatable to TLE in humans, we compared transcriptome changes with recently published  
292 transcriptome changes in TLE patients. This included a study analysing changes in sclerotic  
293 hippocampi vs. neocortex of TLE patients<sup>12</sup> and a study analysing gene expression changes in  
294 cortical tissue from patients with mTLE<sup>14</sup> (**Table S2**). Here we found a very strong  
295 correlation between transcriptome changes identified in the IAKA mouse model during  
296 established epilepsy with transcriptome changes observed in TLE patients (hippocampus and  
297 cortex) (**Fig. 2C**). Similarly, to the IAKA model, there was also a strong correlation of  
298 dysregulated genes between the IHKA model and TLE patients (**Fig. S2A**). In contrast, the  
299 transcriptional profile differed greatly when comparing between human TLE and expression

300 changes 8 h following IAKA-induced SE (**Fig. S2B**). Finally, we also compared  
301 transcriptome profiles between the i.p pilocarpine mouse model and TLE patients. Although  
302 there was a good overlap among down-regulated genes between pilocarpine-injected mice  
303 and TLE patients, this correlation was lost among up-regulated genes. Moreover, the  
304 magnitude of enrichments was minor when compared to both KA mouse models (**Fig. S2C**),  
305 suggesting KA mouse models reflecting closer molecular changes that occur in the brain of  
306 TLE patients.

307

### 308 *Suppressed calcium signalling as a common feature across experimental models of* 309 *epilepsy and TLE patients*

310 To identify pathways and functional groups of genes affected by expression changes  
311 in the IAKA mouse model, differentially expressed transcripts were analyzed by GO terms  
312 using the bioinformatic tool DAVID.<sup>39</sup> This revealed that post-SE up-regulated genes are  
313 mainly associated with signalling pathways (*e.g.*, *MAPK*, *PI3K-Akt*) and down-regulated  
314 genes with metabolism and synaptic transmission (**Fig. 3A** and **Table S3**). At 14 days post-  
315 SE when epilepsy was established, up-regulated genes are highly enriched in pathways linked  
316 to waste removal (*e.g.*, *Phagosome*, *Lysosome*) and down-regulated genes are mainly linked  
317 to pathways controlling synaptic transmission (**Fig. 3A**), similar to down-regulated genes  
318 post-SE (**Fig. 3A**, **Table S3**).

319 GO term analysis of dysregulated genes shared between the IAKA mouse model  
320 (established epilepsy) and TLE patients found a significant enrichment of genes linked to  
321 intracellular signalling (*e.g.*, *PI3K-Akt*, *MAPK*, *TGF- $\beta$* ) and lysosome activity among up-  
322 regulated genes and genes associated with synaptic transmission (*e.g.*, *Calcium signalling*,  
323 *Long-term potentiation*) among down-regulated genes (**Fig. 3B**). Most notably, genes

324 enriched in *Calcium signaling* were significantly affected in all three conditions (**Fig. 3A,B**  
325 and **Table S3**).

326 To further assess whether the enrichment of down-regulated genes involved in  
327 calcium signalling is a common response across different models, GO terms of altered  
328 transcripts were analyzed in all three animal models (KA, pilocarpine) and TLE patients.<sup>12, 14</sup>  
329 This confirmed *Calcium signalling* being a common pathway suppressed in mouse models of  
330 epilepsy and TLE patients (**Fig. 3C, Table S3**). Down-regulated genes involved in *Calcium*  
331 *signaling* and altered post-SE and in human TLE are shown in **Table 1**. Microarray results  
332 were confirmed via single qRT-PCR analysis of selected down-regulated transcripts involved  
333 in *Calcium signalling* either unique to IAKA-induced SE (**Fig. 3D**) or common between SE  
334 and epilepsy (**Fig. 3E**).

335 In summary, our results reveal overlap of several altered pathways between the IAKA  
336 mouse model and human TLE, particularly genes linked to calcium signaling, thereby  
337 identifying possible novel treatment targets for epilepsy.

338

339 *CREB is a major transcription factor controlling gene transcription following*  
340 *intraamygdala status epilepticus and during epilepsy*

341 Analysis via the Ingenuity Pathway Analysis (IPA®)<sup>37</sup> predicted several transcription  
342 factors to regulate gene expression changes post-SE and during epilepsy. Most notably, the  
343 majority of identified transcription factors are unique to SE or epilepsy (*e.g.*, TRP53 and FOS  
344 post-SE), confirming the limited overlap of differently expressed genes between conditions.  
345 Some transcription factors were, however, predicted to control gene expression in both  
346 conditions, including MYC (up-regulated genes post-SE and during epilepsy) and CREB1,  
347 linked to both up- and down-regulated genes under both conditions (**Fig. 4A**).

348 To test whether CREB1 has a role during seizure-induced pathology in the IAKA  
349 mouse model, mice were treated i.c.v. with the CREB1-specific inhibitor 666-15<sup>30</sup> 10 min  
350 before IAKA injection and 1 h after treatment with lorazepam (**Fig. 4B**). Demonstrating  
351 CREB1 regulating the expression of genes linked to *Calcium signalling*, both *CamK4* and  
352 *Grm5* transcripts, down-regulated post-SE, were increased in mice treated with the CREB1  
353 inhibitor 666-15 when compared to vehicle-injected mice 8 h post-SE (**Fig. 4C**). Suggesting a  
354 functional role for CREB1 during IAKA-induced SE, mice treated with the CREB1 inhibitor  
355 666-15 experienced less severe seizures during SE as evidenced by a reduction in behavioural  
356 seizures (**Fig. 4D**), lower seizure total power (**Fig. 4E-F**) and lower transcript level of the  
357 neuronal activity-regulated gene *c-Fos* post-SE (**Fig. 4G**).

358 Thus, our results demonstrate that the IAKA model is a valid model to screen for and  
359 test novel anticonvulsive and antiepileptic drugs.

360

361

## 362 **Discussion**

363 Here, by using a genome-wide gene expression analysis of the hippocampal  
364 transcriptome post-IAKA-induced SE, we demonstrate that the IAKA mouse model mimics  
365 closely molecular changes in the brain of patients with TLE once epilepsy is established and  
366 therefore represents a valid model for the testing of novel antiepileptogenic drug targets.

367 If we are to identify potential anti-epileptogenic and disease-modifying treatments for  
368 drug-resistant epilepsy, then the models we use must phenocopy the human pathophysiology.  
369 Large-scale changes in gene expression caused by injuries to the brain (*e.g.*, traumatic brain  
370 injury, SE) are widely recognized to contribute to the development of epilepsy.<sup>5, 7, 40</sup> Using an  
371 arsenal of different experimental models of acquired epilepsy, we have now detailed  
372 knowledge of the disease-specific expression changes occurring in most of these models and

373 of the molecular machinery driving these changes including transcriptional and post-  
374 transcriptional mechanisms.<sup>6, 10, 41-43</sup> We have now extended this data by characterizing  
375 expression changes in the hippocampus of the IAKA mouse model<sup>19</sup> during both SE and  
376 epilepsy.

377         A first result of our microarray analysis is that gene expression changes are much  
378 more prominent post-SE when compared to established epilepsy. This is in line with previous  
379 studies using models of SE induced via other chemoconvulsants.<sup>8, 10</sup> Another result in  
380 agreement with previous studies is the fact that functional profiles are broadly unique to each  
381 condition.<sup>8, 10</sup> While these findings are not surprising, they confirm the importance of  
382 transcriptional changes during the initial insult which may initiate a cascade of pathological  
383 changes leading eventually to the development of epilepsy. The reason for this initial surge in  
384 gene expression changes is most likely due to the increased neuronal excitability experienced  
385 during SE. Why SE and epilepsy lead to the dysregulation of a different gene pool remains  
386 elusive. The most obvious explanations include differences in seizure severity (SE vs.  
387 spontaneous seizure), time-point of tissue analysis relative to seizures and underlying  
388 pathology (*i.e.*, acute neurodegeneration vs. chronically diseased brain). Interestingly, genes  
389 dysregulated during both conditions are either up- or down-regulated, suggesting some  
390 common regulatory mechanisms during both SE and epilepsy.

391         Our pathway analysis of genes dysregulated in the IAKA model showed in particular  
392 genes linked to signalling pathways to be enriched among up-regulated genes and genes  
393 associated with metabolism and synaptic transmission among down-regulated genes post-SE.  
394 This is broadly in line with pathway analysis in other models (*e.g.*, MAPK family)<sup>6, 10</sup> and  
395 suggests different stimuli activating similar pathways. During epilepsy, pathways most  
396 affected in the IKAK model included pathways involved in waste removal (up-regulated) and  
397 synaptic transmission (down-regulated). In particular, genes linked to lysosome activity were



398 among the most affected genes. This is in good agreement with previous studies showing  
399 genes linked to the mTOR pathway to be commonly dysregulated during epilepsy.<sup>8, 10</sup> Of  
400 note, autophagic/lysosomal system-related proteins are increasingly recognized to play an  
401 important role during epilepsy with drugs targeting autophagy reported to modulate seizures  
402 in several models.<sup>44</sup>

403         While we have amassed much data on gene expression in different models, there has  
404 been a paucity of cross-model comparisons. Here, we compared our findings in the IAKA  
405 mouse model with two commonly used mouse models to induce SE and epilepsy (*i.e.*, IHKA  
406 and i.p. pilocarpine). The main findings here were that gene expression changes are much  
407 more similar between both KA mouse models when compared to the pilocarpine model. An  
408 unexpected result was the almost complete overlap between both KA models, post-SE and  
409 during epilepsy. This is even more remarkable, as both models display different pathologies  
410 during and post-SE. This includes severe seizures during IAKA-induced SE with cell death  
411 mainly restricted to the ipsilateral CA3 subfield *vs.* mostly non-convulsive SE and  
412 widespread hippocampal neurodegeneration in the IHKA mouse model.<sup>23</sup> In contrast, when  
413 we compared the IAKA model with the i.p. pilocarpine mouse model, similarities were less  
414 obvious, in particular post-SE. Thus, gene expression changes seem to be more dependent on  
415 chemoconvulsant used than pathology. It is, however, important to keep in mind that  
416 pilocarpine was delivered i.p. in contrast to the intracerebral delivery of KA in the two other  
417 models.

418         One of the main results of our study is the close correlation of gene expression in the  
419 KA models when compared to human TLE. This is an important finding as this strongly  
420 reinforces the rationale for using these models to identify and test novel anti-epileptogenic  
421 drugs. Another important finding is that these similarities are restricted to established  
422 epilepsy and partly lost when we compared human tissue with mouse tissue collected shortly

423 following SE, suggesting established epilepsy in mice is a much better model for TLE. Why  
424 the pilocarpine model shows less similarities with human TLE we do not know. The  
425 pilocarpine model is, however, associated with peripheral immune responses prior to the  
426 induction of SE and most likely reflects a mixture of an ischemic and excitotoxic insult.<sup>45</sup> In  
427 line with a strong overlap in gene expression between the IAKA mouse model and TLE  
428 patients, pathway analysis of common dysregulated genes revealed similar pathways to be  
429 affected when compared to affected pathways during established epilepsy in the IAKA  
430 model. Most notably, calcium signalling is one of the most consistently affected pathways  
431 across models and patients which is consistent with previous reports.<sup>6, 46, 47</sup> The effects of  
432 suppressed calcium signaling remain to be established. It is, however, tempting to speculate  
433 this being a protective mechanism reducing synaptic transmission and thereby  
434 hyperexcitability in brain tissue. Interestingly, calcium signalling was also suppressed in mice  
435 undergoing epileptic preconditioning.<sup>24</sup>

436 Finally, our IPA analysis predicted the cAMP responsive element binding protein  
437 CREB as one of the main up-stream transcription factors regulating gene transcription during  
438 SE and epilepsy. This is in line with previous findings identifying CREB as one of the main  
439 transcription factors in the pilocarpine mouse model.<sup>10</sup> A role for CREB during seizures has  
440 been previously demonstrated with decreased levels of CREB leading to seizure reduction  
441 following pilocarpine in mice.<sup>48</sup> Whether CREB contributes to seizures via the regulation of  
442 calcium signalling warrants, however, further investigation. Interestingly, P53 was predicted  
443 as one of the main transcription factors driving gene transcription post-SE. P53 has  
444 previously been linked to seizure generation and cell death in the IAKA model.<sup>49</sup> While our  
445 IPA analysis has focused primarily on transcription factors, other mechanisms may also  
446 impact on mRNA levels such as microRNAs or mRNA polyadenylation among many  
447 others.<sup>31, 41</sup>

448 Possible limitations of our study include that gene expression has only been analyzed  
449 shortly post-SE and once epilepsy was already established omitting the seizure-free latent  
450 period. The latent period in the IAKA mouse model is, however, almost absent<sup>23</sup> and the  
451 process of epileptogenesis is ongoing beyond the occurrence of the first epileptic seizure.<sup>5</sup>  
452 Moreover, expression profiles have been analyzed using different analysis platforms (*e.g.*,  
453 microarray *vs.* sequencing) and cut-offs for analysis might be different. In addition, time-  
454 points analyzed relative to initial insult differ between animal models. We have, however,  
455 taken into account the different disease timelines of each model (*e.g.*, much longer latent  
456 period in the pilocarpine model compared to the IAKA model).<sup>16, 45</sup> Moreover, some changes  
457 may have been masked by analyzing the whole hippocampus rather than subfields. Previous  
458 studies analysing gene expression in TLE patients have, however, used resected hippocampal  
459 tissue regardless of subfields.

460 In summary, our results demonstrate the IAKA mouse model closely mimicking  
461 human TLE thus providing strong rationale for using the IAKA model to identify potential  
462 targets for disease-modifying treatments.

463

464

## 465 **Acknowledgments**

466 This work was supported by funding from the Health Research Board HRA-POR-2015-1243  
467 to T.E.; Science Foundation Ireland (17/CDA/4708 to T.E and co-funded under the European  
468 Regional Development Fund and by FutureNeuro industry partners 16/RC/3948 to D.C.H);  
469 from the H2020 Marie Skłodowska-Curie Actions Individual Fellowship (796600 to L.D-G  
470 and 753527 to E.B), from the European Union's Horizon 2020 research and innovation  
471 programme under the Marie Skłodowska-Curie grant agreement (No. 766124 to T.E.).  
472 Further support was obtained from: PI2015-2/06-3&PI2018/06-1(ISCIII-CiberNed),

473 SAF2015-65371-R (MINECO/AEI/FEDER, UE) and RTI2018-096322-B-I00  
474 (MCIU/AEI/FEDER, UE) to J.J.L. A.P. was beneficiary of a Spark grant (SNSF) CRSK-  
475 3\_190764/1. We thank the following core facilities: IRB-Functional Genomic and IRB-  
476 Bioinformatics/Biostatistics.

477

#### 478 **Disclosure of conflict of interest**

479 None of the authors has any conflict of interest to disclose.

480

#### 481 **Ethical Publication Statement**

482 We confirm that we have read the Journal's position on issues involved in ethical publication  
483 and affirm that this report is consistent with those guidelines.

484

485

486

487

488

489

490

491

492

493

494

495

496

497

498

## 499 **References**

- 500 1. Bialer M, White HS. Key factors in the discovery and development of new antiepileptic drugs  
501 Nat Rev Drug Discov. 2010 Jan;9:68-82.
- 502 2. Moshe SL, Perucca E, Ryvlin P, Tomson T. Epilepsy: new advances Lancet. 2015 Mar  
503 7;385:884-898.
- 504 3. Thijs RD, Surges R, O'Brien TJ, Sander JW. Epilepsy in adults Lancet. 2019 Feb 16;393:689-  
505 701.
- 506 4. Chang BS, Lowenstein DH. Epilepsy N Engl J Med. 2003 Sep 25;349:1257-1266.
- 507 5. Pitkanen A, Lukasiuk K. Mechanisms of epileptogenesis and potential treatment targets Lancet  
508 Neurol. 2011 Feb;10:173-186.
- 509 6. Gorter JA, van Vliet EA, Aronica E, Breit T, Rauwerda H, Lopes da Silva FH, et al. Potential  
510 new antiepileptogenic targets indicated by microarray analysis in a rat model for temporal lobe  
511 epilepsy J Neurosci. 2006 Oct 25;26:11083-11110.
- 512 7. Wang YY, Smith P, Murphy M, Cook M. Global expression profiling in epileptogenesis: does it  
513 add to the confusion? Brain Pathol. 2010 Jan;20:1-16.
- 514 8. Okamoto OK, Janjoppi L, Bonone FM, Pansani AP, da Silva AV, Scorza FA, et al. Whole  
515 transcriptome analysis of the hippocampus: toward a molecular portrait of epileptogenesis BMC  
516 Genomics. 2010 Apr 8;11:230.
- 517 9. Goldberg EM, Coulter DA. Mechanisms of epileptogenesis: a convergence on neural circuit  
518 dysfunction Nat Rev Neurosci. 2013 May;14:337-349.
- 519 10. Hansen KF, Sakamoto K, Pelz C, Impey S, Obrietan K. Profiling status epilepticus-induced  
520 changes in hippocampal RNA expression using high-throughput RNA sequencing Sci Rep. 2014  
521 Nov 6;4:6930.
- 522 11. Dixit AB, Banerjee J, Srivastava A, Tripathi M, Sarkar C, Kakkar A, et al. RNA-seq analysis of  
523 hippocampal tissues reveals novel candidate genes for drug refractory epilepsy in patients with  
524 MTLE-HS Genomics. 2016 May;107:178-188.
- 525 12. Salman MM, Sheilabi MA, Bhattacharyya D, Kitchen P, Conner AC, Bill RM, et al.  
526 Transcriptome analysis suggests a role for the differential expression of cerebral aquaporins and  
527 the MAPK signalling pathway in human temporal lobe epilepsy Eur J Neurosci. 2017  
528 Sep;46:2121-2132.
- 529 13. Srivastava PK, van Eyll J, Godard P, Mazzuferi M, Delahaye-Duriez A, Van Steenwinckel J, et  
530 al. A systems-level framework for drug discovery identifies Csf1R as an anti-epileptic drug  
531 target Nat Commun. 2018 Sep 3;9:3561.
- 532 14. Guelfi S, Botia JA, Thom M, Ramasamy A, Perona M, Stanyer L, et al. Transcriptomic and  
533 genetic analyses reveal potential causal drivers for intractable partial epilepsy Brain. 2019 Jun  
534 1;142:1616-1630.
- 535 15. Loscher W. Animal Models of Seizures and Epilepsy: Past, Present, and Future Role for the  
536 Discovery of Antiseizure Drugs Neurochem Res. 2017 Jul;42:1873-1888.
- 537 16. Mouri G, Jimenez-Mateos E, Engel T, Dunleavy M, Hatazaki S, Paucard A, et al. Unilateral  
538 hippocampal CA3-predominant damage and short latency epileptogenesis after intra-amygdala  
539 microinjection of kainic acid in mice Brain Res. 2008 Jun 5;1213:140-151.
- 540 17. Wu YP, Siao CJ, Lu W, Sung TC, Frohman MA, Milev P, et al. The tissue plasminogen activator  
541 (tPA)/plasmin extracellular proteolytic system regulates seizure-induced hippocampal mossy  
542 fiber outgrowth through a proteoglycan substrate J Cell Biol. 2000 Mar 20;148:1295-1304.
- 543 18. Li T, Ren G, Lusardi T, Wilz A, Lan JQ, Iwasato T, et al. Adenosine kinase is a target for the  
544 prediction and prevention of epileptogenesis in mice J Clin Invest. 2008 Feb;118:571-582.
- 545 19. Jimenez-Mateos EM, Engel T, Merino-Serrais P, McKiernan RC, Tanaka K, Mouri G, et al.  
546 Silencing microRNA-134 produces neuroprotective and prolonged seizure-suppressive effects  
547 Nat Med. 2012 Jul;18:1087-1094.

- 548 20. Liu G, Gu B, He XP, Joshi RB, Wackerle HD, Rodriguiz RM, et al. Transient inhibition of TrkB  
549 kinase after status epilepticus prevents development of temporal lobe epilepsy *Neuron*. 2013 Jul  
550 10;79:31-38.
- 551 21. Iori V, Iyer AM, Ravizza T, Beltrame L, Paracchini L, Marchini S, et al. Blockade of the IL-  
552 1R1/TLR4 pathway mediates disease-modification therapeutic effects in a model of acquired  
553 epilepsy *Neurobiol Dis*. 2017 Mar;99:12-23.
- 554 22. Colasante G, Qiu Y, Massimino L, Di Berardino C, Cornford JH, Snowball A, et al. In vivo  
555 CRISPRa decreases seizures and rescues cognitive deficits in a rodent model of epilepsy *Brain*.  
556 2020 Mar 1;143:891-905.
- 557 23. Welzel L, Schidlitzki A, Twele F, Anjum M, Loscher W. A face-to-face comparison of the intra-  
558 amygdala and intrahippocampal kainate mouse models of mesial temporal lobe epilepsy and their  
559 utility for testing novel therapies *Epilepsia*. 2020 Jan;61:157-170.
- 560 24. Jimenez-Mateos EM, Hatazaki S, Johnson MB, Bellver-Estelles C, Mouri G, Bonner C, et al.  
561 Hippocampal transcriptome after status epilepticus in mice rendered seizure damage-tolerant by  
562 epileptic preconditioning features suppressed calcium and neuronal excitability pathways  
563 *Neurobiol Dis*. 2008 Dec;32:442-453.
- 564 25. Engel T, Sanz-Rodriguez A, Jimenez-Mateos EM, Concannon CG, Jimenez-Pacheco A, Moran  
565 C, et al. CHOP regulates the p53-MDM2 axis and is required for neuronal survival after seizures  
566 *Brain*. 2013 Feb;136:577-592.
- 567 26. Torres-Peraza JF, Engel T, Martin-Ibanez R, Sanz-Rodriguez A, Fernandez-Fernandez MR,  
568 Esgleas M, et al. Protective neuronal induction of ATF5 in endoplasmic reticulum stress induced  
569 by status epilepticus *Brain*. 2013 Apr;136:1161-1176.
- 570 27. Engel T, Gomez-Sintes R, Alves M, Jimenez-Mateos EM, Fernandez-Nogales M, Sanz-  
571 Rodriguez A, et al. Bi-directional genetic modulation of GSK-3beta exacerbates hippocampal  
572 neuropathology in experimental status epilepticus *Cell Death Dis*. 2018 Sep 20;9:969.
- 573 28. Jimenez-Pacheco A, Mesuret G, Sanz-Rodriguez A, Tanaka K, Mooney C, Conroy R, et al.  
574 Increased neocortical expression of the P2X7 receptor after status epilepticus and anticonvulsant  
575 effect of P2X7 receptor antagonist A-438079 *Epilepsia*. 2013 Sep;54:1551-1561.
- 576 29. Xie F, Li BX, Kassenbrock A, Xue C, Wang X, Qian DZ, et al. Identification of a Potent  
577 Inhibitor of CREB-Mediated Gene Transcription with Efficacious in Vivo Anticancer Activity *J*  
578 *Med Chem*. 2015 Jun 25;58:5075-5087.
- 579 30. Li BX, Gardner R, Xue C, Qian DZ, Xie F, Thomas G, et al. Systemic Inhibition of CREB is  
580 Well-tolerated in vivo *Sci Rep*. 2016 Oct 3;6:34513.
- 581 31. Parras A, Anta H, Santos-Galindo M, Swarup V, Elorza A, Nieto-Gonzalez JL, et al. Autism-like  
582 phenotype and risk gene mRNA deadenylation by CPEB4 mis-splicing *Nature*. 2018  
583 Aug;560:441-446.
- 584 32. Gentleman RC, Carey VJ, Bates DM, Bolstad B, Dettling M, Dudoit S, et al. Bioconductor: open  
585 software development for computational biology and bioinformatics *Genome Biol*. 2004;5:R80.
- 586 33. Ritchie ME, Phipson B, Wu D, Hu Y, Law CW, Shi W, et al. limma powers differential  
587 expression analyses for RNA-sequencing and microarray studies *Nucleic Acids Res*. 2015 Apr  
588 20;43:e47.
- 589 34. Alves M, De Diego Garcia L, Conte G, Jimenez-Mateos EM, D'Orsi B, Sanz-Rodriguez A, et al.  
590 Context-Specific Switch from Anti- to Pro-epileptogenic Function of the P2Y1 Receptor in  
591 Experimental Epilepsy *J Neurosci*. 2019 Jul 3;39:5377-5392.
- 592 35. Motti D, Le Duigou C, Eugene E, Chemaly N, Wittner L, Lazarevic D, et al. Gene expression  
593 analysis of the emergence of epileptiform activity after focal injection of kainic acid into mouse  
594 hippocampus *Eur J Neurosci*. 2010 Oct;32:1364-1379.
- 595 36. Huang da W, Sherman BT, Lempicki RA. Systematic and integrative analysis of large gene lists  
596 using DAVID bioinformatics resources *Nat Protoc*. 2009;4:44-57.
- 597 37. Kramer A, Green J, Pollard J, Jr., Tugendreich S. Causal analysis approaches in Ingenuity  
598 Pathway Analysis *Bioinformatics*. 2014 Feb 15;30:523-530.
- 599 38. Alves M, Kenny A, de Leo G, Beamer EH, Engel T. Tau Phosphorylation in a Mouse Model of  
600 Temporal Lobe Epilepsy *Front Aging Neurosci*. 2019;11:308.

- 601 39. Huang C, Chi XS, Li R, Hu X, Xu HX, Li JM, et al. Inhibition of P2X7 Receptor Ameliorates  
602 Nuclear Factor-Kappa B Mediated Neuroinflammation Induced by Status Epilepticus in Rat  
603 Hippocampus *J Mol Neurosci*. 2017 Oct;63:173-184.
- 604 40. Klein P, Dingledine R, Aronica E, Bernard C, Blumcke I, Boison D, et al. Commonalities in  
605 epileptogenic processes from different acute brain insults: Do they translate? *Epilepsia*. 2018  
606 Jan;59:37-66.
- 607 41. Henshall DC, Hamer HM, Pasterkamp RJ, Goldstein DB, Kjems J, Prehn JHM, et al.  
608 MicroRNAs in epilepsy: pathophysiology and clinical utility *Lancet Neurol*. 2016 Dec;15:1368-  
609 1376.
- 610 42. Engel T, Martinez-Villarreal J, Henke C, Jimenez-Mateos EM, Sanz-Rodriguez A, Alves M, et  
611 al. Spatiotemporal progression of ubiquitin-proteasome system inhibition after status epilepticus  
612 suggests protective adaptation against hippocampal injury *Mol Neurodegener*. 2017 Feb  
613 24;12:21.
- 614 43. Srivastava PK, Bagnati M, Delahaye-Duriez A, Ko JH, Rotival M, Langley SR, et al. Genome-  
615 wide analysis of differential RNA editing in epilepsy *Genome Res*. 2017 Mar;27:440-450.
- 616 44. Fassio A, Falace A, Esposito A, Aprile D, Guerrini R, Benfenati F. Emerging Role of the  
617 Autophagy/Lysosomal Degradative Pathway in Neurodevelopmental Disorders With Epilepsy  
618 *Front Cell Neurosci*. 2020;14:39.
- 619 45. Curia G, Longo D, Biagini G, Jones RS, Avoli M. The pilocarpine model of temporal lobe  
620 epilepsy *J Neurosci Methods*. 2008 Jul 30;172:143-157.
- 621 46. Elliott RC, Miles MF, Lowenstein DH. Overlapping microarray profiles of dentate gyrus gene  
622 expression during development- and epilepsy-associated neurogenesis and axon outgrowth *J*  
623 *Neurosci*. 2003 Mar 15;23:2218-2227.
- 624 47. Lauren HB, Lopez-Picon FR, Brandt AM, Rios-Rojas CJ, Holopainen IE. Transcriptome analysis  
625 of the hippocampal CA1 pyramidal cell region after kainic acid-induced status epilepticus in  
626 juvenile rats *PLoS One*. 2010 May 20;5:e10733.
- 627 48. Zhu X, Han X, Blendy JA, Porter BE. Decreased CREB levels suppress epilepsy *Neurobiol Dis*.  
628 2012 Jan;45:253-263.
- 629 49. Engel T, Tanaka K, Jimenez-Mateos EM, Caballero-Caballero A, Prehn JH, Henshall DC. Loss  
630 of p53 results in protracted electrographic seizures and development of an aggravated epileptic  
631 phenotype following status epilepticus *Cell Death Dis*. 2010 Oct 7;1:e79.

632

633

634 **Figure Legends**

635 **Figure 1. Gene expression analysis post-intraamygdala KA-induced status epilepticus**  
636 **and during epilepsy.** (A) Schematic showing experimental design using the intraamygdala  
637 kainic acid (IACA)-induced SE mouse model. Mice were euthanatized at two time-points: 8  
638 h post-SE (acute) and 14 days (chronic epilepsy). Ipsilateral hippocampi were removed and  
639 transcript levels analyzed via microarray. (B) Volcano plot of genes analyzed by microarray.  
640 The X-axis represents the  $\log_2$  ratio of gene expression levels and the Y-axis the adjusted  $P$ -  
641 value based on  $-\log_{10}$ . The red dashed line denotes the significant level ( $P \leq 0.01$ ). Purple  
642 dots represent genes with most dramatic expression changes. (C) Heatmap of genes showing  
643 the most dramatic expression changes (down-regulated fold change (FC)  $< -1.75$  blue; up-  
644 regulated FC  $> 4$  yellow), post-SE (acute) (top part) and during chronic epilepsy (bottom  
645 part). (D) Bar chart representing the number of dysregulated genes post-SE and in chronic  
646 epilepsy. (E) Venn diagram showing overlap of differentially expressed genes at the two  
647 time-points analyzed. (F) Comparison of differentially expressed genes post-SE and during  
648 epilepsy. The Y-axis represents the fold change enrichment and X-axis shows the different  
649 gene regulation post-SE (8 h). Colours show the different gene regulation during epilepsy (14  
650 days). One-sided Fisher's exact test ( $***P < 0.001$ ).

651

652 **Figure 2. Comparison of genes undergoing expression changes in experimental models**  
653 **of epilepsy and TLE patients.** Graphs showing comparison of dysregulated genes in the  
654 hippocampus of (A) mice subjected to IACA and intraperitoneal (i.p.) pilocarpine and (B)  
655 mice subjected to IACA and IHKA post-SE and during chronic epilepsy. (C) Comparison of  
656 dysregulated genes in hippocampus of IACA (14 days) and hippocampi from patients with  
657 TLE (left panel) and cortex from patients with mTLE (right panel). Up-regulated genes are  
658 presented in yellow in both conditions and down-regulated genes are presented in blue.



659 Overlap: Representation Factor (RF) > 2 and  $P < 0.05$ , and dissimilar RF < 0.5 and  $P < 0.05$ .

660 Hypergeometric test.

661

662 **Figure 3. Gene Ontology (GO) analysis and validation of microarray results.** Gene count

663 histogram from GO analysis using DAVID resources of differentially expressed genes in (A)

664 post-SE and in epilepsy, (B) TLE patients and IAKA epileptic mice common dysregulated

665 genes. (C) Number of genes of calcium signalling pathway in down-regulated genes in IAKA

666 and IHKA mouse models of epilepsy, in TLE patients (hippocampus and cortex) and in the

667 i.p. pilocarpine model of epilepsy (one-sided Fisher's exact test). (D-E) mRNA level analysis

668 by qRT-PCR of down-regulated genes involved in calcium signalling, (D) following SE

669 (control n= 4/7, post-SE n= 4/6) and (E) at both time-points (control n = 7 (*Ltp1*) and 8

670 (*CamK4*), post-SE n = 7 (*Ltp1*) and 9 (*CamK4*); control n = 8, epilepsy n = 10). Two-sided

671 unpaired t-test. Data are mean  $\pm$  S.E.M. \*  $P < 0.05$  \*\*  $P < 0.01$  \*\*\*  $P < 0.001$ .

672

673 **Figure 4. CREB1 as up-stream transcription factor during status epilepticus and**

674 **epilepsy.** (A) Prediction of transcription factors involved in gene upregulation (yellow) and

675 downregulation (blue) post-SE and during epilepsy by using Ingenuity Pathway Analysis

676 (IPA®). Of note, transcription factor CREB1 is one of the transcription factors with highest

677 amount of predicted target genes among up- and down-regulated gene pool during both

678 conditions, post-SE and during epilepsy. (B) Schematic of experimental design to test

679 CREB1 inhibition on SE. Mice subjected to IAKA were treated i.c.v. with the CREB1

680 inhibitor 666-15 (2 nmol) 10 min before KA injection and 1 h after lorazepam treatment. (C)

681 Graphs showing increased mRNA levels of the two CREB1 target genes, *CamK4* and *Grm5*.

682 (D) Behavioural severity of seizures (mean Racine score) scored each 5 min and total score,

683 in mice subjected to IAKA treated with vehicle (Veh) (n = 4) and treated with the CREB1

684 inhibitor 666-15 (n = 5). **(E)** Representative EEG recordings presented as heat maps of  
685 frequency and amplitude data showing reduced seizure severity in mice treated with the  
686 CREB1 inhibitor 666-15. **(F)** Bar chart showing decreased EEG total power during SE in  
687 mice treated with the CREB1 inhibitor 666-15 (n = 9) when compared to vehicle-treated mice  
688 (n = 7). **(G)** Reduced transcript levels of the neuronal activity-regulated gene *c-Fos* in mice  
689 treated with the CREB1 inhibitor 666-15 when compared to vehicle-treated mice 8 h post-  
690 lorazepam injection (n = 5 per group). **(C-G)** Two-sided unpaired t-test. Data are mean  $\pm$   
691 S.E.M. \*  $P < 0.05$ .

692

693 **Supplementary Figure 1. Validation of differently expressed genes detected via**  
694 **microarray analysis.** **(A)** Log<sub>2</sub> fold change of mRNA levels obtained by microarray analysis  
695 and **(B)** mRNA levels analysed by qRT-PCR and normalized to *β-Actin* of genes which are  
696 up-regulated post-SE and during epilepsy. Two-sided unpaired t-test. Data are mean  $\pm$  S.E.M.  
697 \*  $P < 0.05$ , \*\*  $P < 0.01$ , \*\*\*  $P < 0.001$ .

698

699 **Supplementary Figure 2. Additional comparisons of dysregulated genes between animal**  
700 **models of epilepsy and patients.** Graphs showing the comparison of dysregulated genes in  
701 TLE patients (hippocampus (left) and cortex (right)) with **(A)** the IHKA mouse model during  
702 epilepsy (15 days post-KA injection), **(B)** the IAKA mouse model following post-SE (8 h)  
703 and **(C)** the i.p. pilocarpine epilepsy model (6 weeks post-pilocarpine injection). Up-regulated  
704 genes common between two conditions are presented in yellow and down-regulated genes  
705 common between conditions in blue. Overlap: Representation Factor (RF)  $> 2$  and  $P < 0.05$ ,  
706 and dissimilar RF  $< 0.5$  and  $P < 0.05$ . Hypergeometric test.

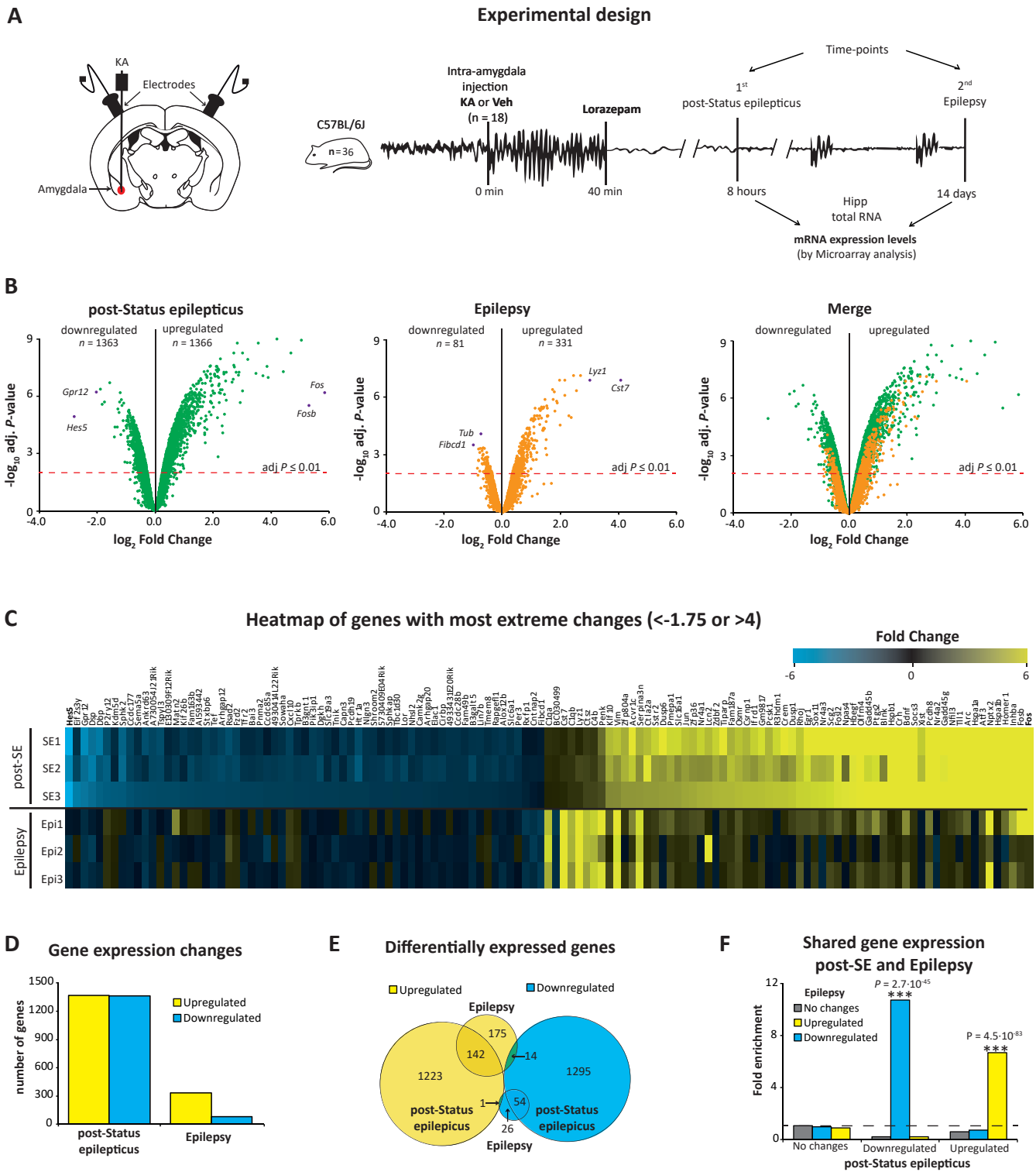


Figure 1

### Comparison of gene expression changes

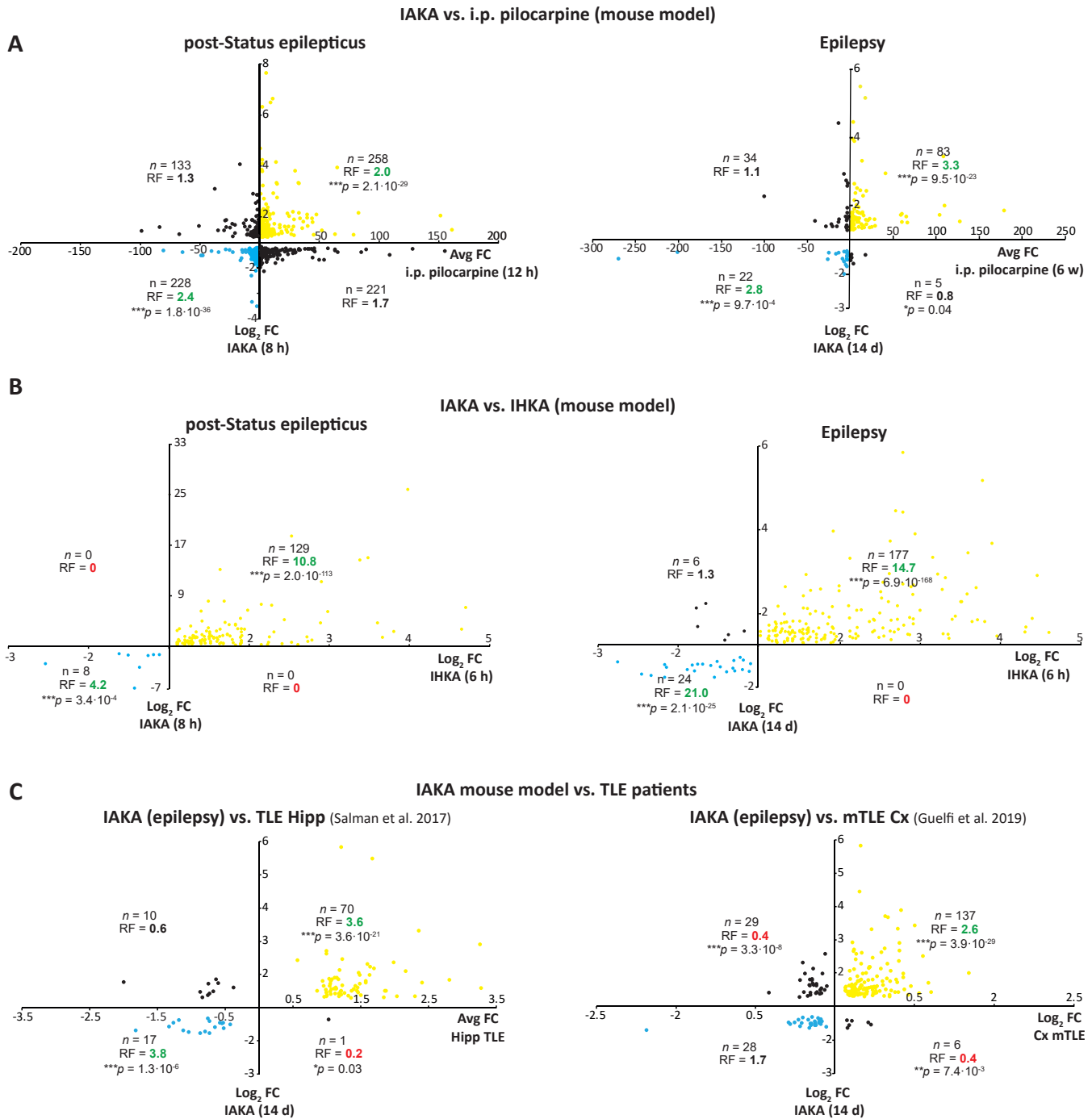
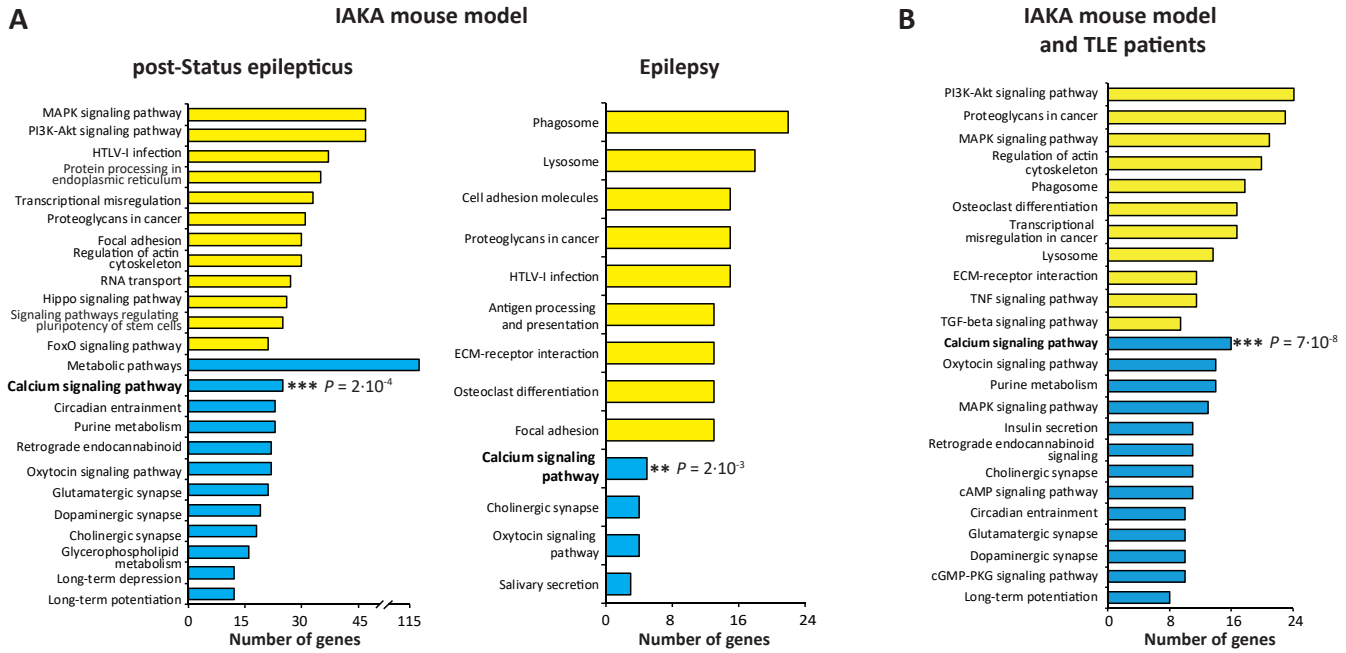
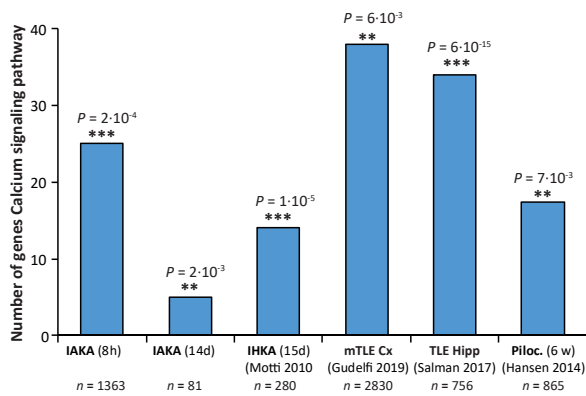


Figure 2

### GO terms of differentially expressed genes - KEGG Pathways



**C** Calcium signaling pathway (downregulated genes)



**Validation via qRT-PCR**

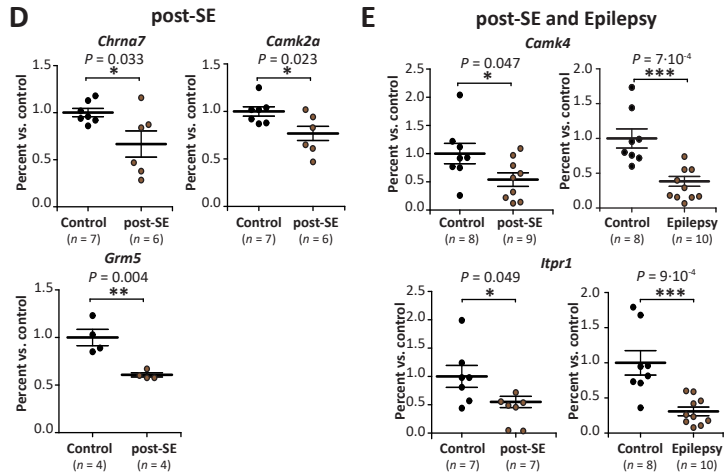


**Figure 3**

### Calcium signalling (down-regulated genes) - mouse models of epilepsy and/or TLE patients

Symbol	Gene Name	IAKA	TLE human	i.p. Pilocarpine	IHKA
ADCY1	Adenylate cyclase 1 (brain)	post-SE	Cx & Hipp	--	--
ADCY2	Adenylate cyclase 2 (brain)	--	Hipp	post-SE & Epilepsy	Epilepsy
ADCY3	Adenylate cyclase 3	--	Cx	--	--
ADCY9	Adenylate cyclase 9	post-SE	Cx	--	--
ADRA1B	Adrenoceptor $\alpha$ 1B	--	Hipp	--	--
ADRA1D	Adrenoceptor $\alpha$ 1D	--	Cx	--	--
ADRB1	Adrenoceptor $\beta$ 1	--	Cx & Hipp	--	--
ATP2A2	Atpase, Ca <sup>++</sup> transporting, cardiac muscle, slow twitch 2	--	--	post-SE & Epilepsy	--
ATP2B1	Atpase, Ca <sup>++</sup> transporting, plasma membrane 1	--	Cx & Hipp	post-SE & Epilepsy	--
ATP2B2	Atpase, Ca <sup>++</sup> transporting, plasma membrane 2	--	Cx & Hipp	post-SE & Epilepsy	--
ATP2B3	Atpase, Ca <sup>++</sup> transporting, plasma membrane 3	post-SE	Cx	Epilepsy	--
BDKRB2	Bradykinin receptor B2	--	Hipp	--	--
CACNA1B	Calcium channel, voltage-dependent, N type, $\alpha$ 1B subunit	--	Hipp	post-SE	--
CACNA1C	Calcium channel, voltage-dependent, L type, $\alpha$ 1C subunit	--	Cx	post-SE	--
CACNA1D	Calcium channel, voltage-dependent, L type, $\alpha$ 1D subunit	post-SE	--	post-SE	--
CACNA1E	Calcium channel, voltage-dependent, R type, $\alpha$ 1E subunit	--	--	post-SE	--
CACNA1F	Calcium channel, voltage-dependent, L type, $\alpha$ 1F subunit	--	Hipp	--	--
CACNA1G	Calcium channel, voltage-dependent, T type, $\alpha$ 1G subunit	--	Cx & Hipp	--	--
CACNA1H	Calcium channel, voltage-dependent, T type, $\alpha$ 1H subunit	--	--	post-SE & Epilepsy	--
CACNA1I	Calcium channel, voltage-dependent, T type, $\alpha$ 1I subunit	--	Cx	--	--
CAMK2A	Calcium/calmodulin-dependent protein kinase II $\alpha$	post-SE	Cx & Hipp	post-SE & Epilepsy	--
CAMK2B	Calcium/calmodulin-dependent protein kinase II $\beta$	--	Cx	post-SE & Epilepsy	--
CAMK2G	Calcium/calmodulin-dependent protein kinase II $\gamma$	post-SE	Cx	post-SE	--
CAMK4	Calcium/calmodulin-dependent protein kinase IV	post-SE & Epilepsy	Cx	--	--
CCKBR	Cholecystokinin B receptor	--	--	--	Epilepsy
CD38	CD38 molecule	--	--	post-SE	--
CHRM1	Cholinergic receptor, muscarinic 1	--	Hipp	post-SE & Epilepsy	--
CHRM2	Cholinergic receptor, muscarinic 2	--	Hipp	--	--
CHRM3	Cholinergic receptor, muscarinic 3	Epilepsy	Hipp	--	--
DRD5	Dopamine receptor D5	--	Hipp	--	--
EDNRB	Endothelin receptor type B	--	--	post-SE	--
ERBB4	V-erb-b2 avian erythroblastic leukemia viral oncogene h4	post-SE	--	--	--
GNA11	Guanine nucleotide binding protein, $\alpha$ 11 (Gq class)	--	Cx	post-SE & Epilepsy	--
GNA15	Guanine nucleotide binding protein, $\alpha$ 15	--	Cx	--	--
GNAL	Guanine nucleotide binding protein, $\alpha$ activating	--	--	post-SE & Epilepsy	--
GNAQ	Guanine nucleotide binding protein, q polypeptide	post-SE	--	post-SE	--
GNAS	GNAS complex locus	--	--	post-SE & Epilepsy	--
GRIN1	Glutamate receptor, ionotropic, N-methyl D-aspartate 1	--	Hipp	Epilepsy	--
GRIN2A	Glutamate receptor, ionotropic, N-methyl D-aspartate 2A	--	Cx & Hipp	--	--
GRM1	Glutamate receptor, metabotropic 1	--	--	post-SE	Epilepsy
GRM5	Glutamate receptor, metabotropic 5	post-SE	Hipp	--	--
HTR2A	5-hydroxytryptamine receptor 2A, G protein-coupled	--	Hipp	--	--
HTR4	5-hydroxytryptamine receptor 4, G protein-coupled	--	Hipp	--	--
HTR5A	5-hydroxytryptamine receptor 5A, G protein-coupled	--	Hipp	--	--
ITPKA	Inositol-trisphosphate 3-kinase A	post-SE	Cx & Hipp	--	Epilepsy
ITPKB	Inositol-trisphosphate 3-kinase B	--	--	post-SE	--
ITPR1	Inositol 1,4,5-trisphosphate receptor, type 1	post-SE & Epilepsy	Cx & Hipp	post-SE	Epilepsy
ITPR2	Inositol 1,4,5-trisphosphate receptor, type 2	--	--	post-SE	--
NOS1	Nitric oxide synthase 1 (neuronal)	post-SE	--	--	Epilepsy
NOS2	Nitric oxide synthase 2, inducible	--	Cx & Hipp	--	--
NTSR1	Neurotensin receptor 1 (high affinity)	--	Hipp	--	Epilepsy
ORAI2	ORAI calcium release-activated calcium modulator 2	--	--	post-SE	--
ORAI3	ORAI calcium release-activated calcium modulator 3	post-SE	--	--	--
P2RX5	Purinergic receptor P2X, ligand-gated ion channel, 5	--	--	--	Epilepsy
P2RX6	Purinergic receptor P2X, ligand-gated ion channel, 6	--	Cx	--	--
PDE1A	Phosphodiesterase 1A, calmodulin-dependent	--	--	post-SE	Epilepsy
PDE1B	Phosphodiesterase 1B, calmodulin-dependent	post-SE	Hipp	post-SE & Epilepsy	--
PHKA2	Phosphorylase kinase, $\alpha$ 2 (liver)	post-SE	--	--	--
PHKB	Phosphorylase kinase, beta	--	--	Epilepsy	--
PHKG1	Phosphorylase kinase, $\gamma$ 1 (muscle)	post-SE	--	--	--
PLCB1	Phospholipase C, $\beta$ 1 (phosphoinositide-specific)	post-SE	Cx & Hipp	post-SE	--
PLCB3	Phospholipase C, $\beta$ 3 (phosphatidylinositol-specific)	--	--	post-SE	--
PLCB4	Phospholipase C, $\beta$ 4	--	Cx	post-SE	--
PLCD4	Phospholipase C, delta 4	--	Hipp	--	--
PLCG1	Phospholipase C, $\gamma$ 1	--	--	post-SE & Epilepsy	--
PPIF	Peptidylprolyl isomerase F	--	--	Epilepsy	--
PPP3CA	Protein phosphatase 3, catalytic subunit, $\alpha$ isozyme	post-SE	Cx & Hipp	post-SE & Epilepsy	--
PPP3CB	Protein phosphatase 3, catalytic subunit, $\beta$ isozyme	--	Hipp	--	--
PPP3CC	Protein phosphatase 3, catalytic subunit, $\gamma$ isozyme	--	Cx	--	--
PPP3R1	Protein phosphatase 3, regulatory subunit B, $\alpha$	--	Cx & Hipp	post-SE & Epilepsy	--
PRKACA	Protein kinase, camp-dependent, catalytic, $\alpha$	--	Cx	Epilepsy	--
PRKCA	Protein kinase C, $\alpha$	--	Cx	post-SE & Epilepsy	--
PRKCB	Protein kinase C, $\beta$	--	Cx & Hipp	post-SE	--
PTGER1	Prostaglandin E receptor 1 (subtype EP1), 42kda	--	Cx	--	--
PTGER3	Prostaglandin E receptor 3 (subtype EP3)	--	Hipp	--	--
PTK2B	Protein tyrosine kinase 2 $\beta$	post-SE & Epilepsy	Cx	post-SE & Epilepsy	Epilepsy
RYR1	Ryanodine receptor 1 (skeletal)	post-SE	--	--	--
RYR2	Ryanodine receptor 2 (cardiac)	post-SE	Cx & Hipp	post-SE	Epilepsy
RYR3	Ryanodine receptor 3	Epilepsy	--	post-SE	--
SLC25A4	Solute carrier family 25, member 4	--	Cx	Epilepsy	--
SLC8A1	Solute carrier family 8, member 1	--	Cx	post-SE & Epilepsy	Epilepsy
SLC8A2	Solute carrier family 8 (Na/Ca exchanger), member 2	--	--	Epilepsy	--
SPHK2	Sphingosine kinase 2	post-SE	Cx	post-SE	--
TACR1	Tachykinin receptor 1	--	Cx	--	--
TACR3	Tachykinin receptor 3	--	--	--	Epilepsy
TRHR	Thyrotropin-releasing hormone receptor	--	--	--	Epilepsy

Table 1

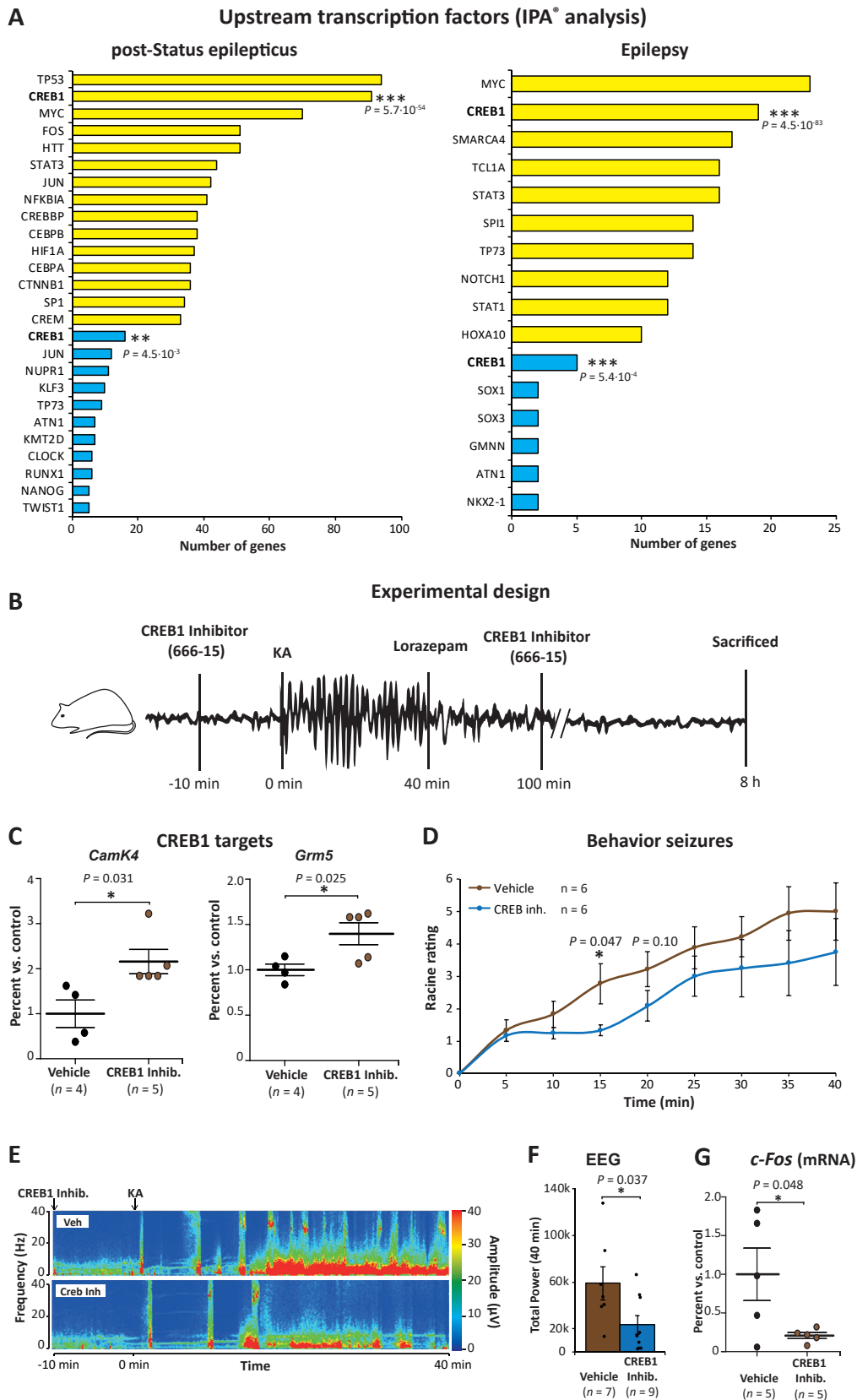


Figure 4